

Parity nonconservation in neutron capture on ^{113}Cd

S. J. Seestrom,¹ J. D. Bowman,¹ B. E. Crawford,^{2,3,*} P. P. J. Delheij,⁴ C. M. Frankle,¹ C. R. Gould,^{3,5} D. G. Haase,^{3,5} M. Iinuma,^{6,†} J. N. Knudson,¹ P. E. Koehler,^{1,‡} L. Y. Lowie,^{3,5} A. Masaike,⁶ Y. Masuda,⁷ Y. Matsuda,⁶ G. E. Mitchell,^{3,5} S. I. Penttilä,¹ Yu. P. Popov,⁸ H. Postma,⁹ N. R. Roberson,^{2,3} E. I. Sharapov,⁸ H. M. Shimizu,^{7,§} D. A. Smith,¹ S. L. Stephenson,^{3,5,**} Y. F. Yen,¹ and V. W. Yuan¹

¹Los Alamos National Laboratory, Los Alamos, New Mexico 87545

²Duke University, Durham, North Carolina 27708

³Triangle Universities Nuclear Laboratory, Durham, North Carolina 27708

⁴TRIUMF, Vancouver, British Columbia, Canada V6T 2A3

⁵North Carolina State University, Raleigh, North Carolina 27965

⁶Physics Department, Kyoto University, Kyoto 606-01, Japan

⁷National Laboratory of High Energy Physics, Tsukuba-shi 305, Japan

⁸Joint Institute for Nuclear Research, Dubna, 141980, Russia

⁹Delft University of Technology, Delft, 2600 GA, the Netherlands

(Received 2 December 1997)

Parity nonconservation was studied for 23 p -wave resonances in ^{113}Cd up to $E_n = 500$ eV at the LANSCE pulsed neutron source using a longitudinally polarized neutron beam and the time-of-flight method. The helicity dependence of the total neutron capture cross section was measured with an enriched ^{113}Cd target and with a target of natural cadmium. Parity violating effects were observed for several resonances in ^{113}Cd and ^{111}Cd . A root-mean-square value of the parity nonconserving matrix element $M_{J=1} = 2.9_{-0.9}^{+1.3}$ meV was obtained for the spin $J=1$ levels in the compound nucleus ^{114}Cd . This result from the $3p$ -peak region of the neutron strength function is compared with the parity violation results for nuclei from the $4p$ -peak region. [S0556-2813(98)02210-9]

PACS number(s): 25.40.Ny, 24.80.+y, 11.30.Er, 27.60.+j

I. INTRODUCTION

The significant experimental progress achieved to date in the measurement of parity violation (PV) in neutron p -wave resonances is reviewed in Refs. [1–4]. These reviews emphasize the large size of the measured longitudinal asymmetries and the need for further study of this phenomenon.

In conformity with the definition presented in the pioneering work of Alfimenkov *et al.* [5], the parity nonconserving (PNC) longitudinal asymmetry $\mathcal{P}(E)$ is the fractional difference between the p -wave resonance cross sections for the helicity states plus (+) and minus (–):

$$\mathcal{P}(E) = \frac{\sigma_p^+(E) - \sigma_p^-(E)}{\sigma_p^+(E) + \sigma_p^-(E)}, \quad (1.1)$$

where $[\sigma_p^+(E) + \sigma_p^-(E)]/2 = \sigma_p(E)$ is the p -wave part of the total neutron cross section

*Present address: North Carolina State University, Raleigh, NC 27695-8202 and Gettysburg College, Gettysburg, PA 17325.

†Present address: Hiroshima University, Hiroshima-Ken, 739, Japan.

‡Present address: Oak Ridge National Laboratory, Oak Ridge, TN 37831.

§Present address: RIKEN, Saitama 351-01, Japan

**Present address: Gettysburg College, Gettysburg, PA 17325.

$$\sigma_p(E) = \frac{\pi}{k^2} \frac{g_J \Gamma_{np} \Gamma_p}{(E - E_p)^2 + (\Gamma_p/2)^2}, \quad g_J = \frac{2J+1}{2(2I+1)}. \quad (1.2)$$

Here Γ_p is the total width of the resonance, Γ_{np} is the neutron width, E_p is the resonance energy, J is the spin of the compound nuclear resonance, and I is the angular momentum of the target. In the vicinity of p -wave resonance, the numerator in Eq. (1.1) behaves nearly resonantly [6,7], so that the perturbation-theory expression for the constant asymmetry

$$\mathcal{P}(E_p) = R \sum_s \frac{2V_{sp}(J) g_s(E_p)}{E_s - E_p g_p(E_p)}, \quad (1.3)$$

$$R = \frac{g_{p(1/2)}}{\sqrt{g_{p(1/2)}^2 + g_{p(3/2)}^2}}$$

can be used for each p -wave resonance exhibiting parity violation. Here V_{sp} is the matrix element of the weak interaction between a p -wave resonance at E_p and an s -wave resonance at energy E_s with the same spin J . The quantities g_p and g_s (defined as $g = \pm \sqrt{\Gamma_n}$) are the neutron width amplitudes of the corresponding states, and R characterizes the relative contribution of the partial neutron amplitude $g_{p(1/2)}$ of a p -wave resonance in the representation of the total angular momentum j ($j=1/2$ and $3/2$). According to the statistical approach to the compound nucleus, the weak matrix elements $V_{sp}(J)$ are uncorrelated Gaussian variables with zero mean and variance $\langle V_{sp}^2(J) \rangle$. The amplitudes $g_s(E_s)$,

$g_p(E_p)$ also are uncorrelated zero-mean Gaussian variables. The matrix elements $V_{sp}(J)$ are, in principle, the quantities under study, while the presence of other random variables is accounted for by the use of spectroscopic information or by an appropriate averaging. However, it is impossible to determine each of the matrix elements V_{sp} for a given p level p because several s -wave resonances can contribute to the value of $\mathcal{P}(E_p)$ for this level. Instead, adopting the statistical approach, we assume that the relevant compound nucleus amplitudes satisfy the ergodic hypothesis [8–10] and that the quantity V_{sp} is a mean zero Gaussian variable with a variance M_J^2 which is defined as the expectation value of V_{sp}^2 over an ensemble of sp -compound states with a given J : $M_J^2 = E(|V_{sp}|^2)$. It is possible to obtain M_J directly by the likelihood analysis of measured asymmetries $\mathcal{P}(E_p)$; such an analysis was performed for the first time in Ref. [8].

In analogy with time reversal [11] and isospin symmetry [12,13] violations, the corresponding spreading width Γ_w of the weak interaction is introduced

$$\Gamma_w = \frac{2\pi M_J^2}{D_J}, \quad (1.4)$$

which is expected to be approximately independent of the atomic mass number A and of the resonance spin J , that is, M_J^2 scales with D_J which is the average level spacing in the compound nucleus of a given spin J for the $l=0$ levels. However, it was proposed in Refs. [14,15] that M_J^2 scales with AD_J as

$$M_J = 1.3 \times 10^{-8} \sqrt{A u_{\text{eff}} D_J}, \quad (1.5)$$

where the quantities M_J , D_J , and the effective excitation energy $u_{\text{eff}} = E_b - \Delta$ (here E_b is the neutron binding energy and Δ is the pairing energy taken from Ref. [16]) have dimensions eV. In Ref. [14] the dynamic enhancement of parity violation is due to the virtual excitation of a giant 0^- resonance by the weak interaction. The mass dependence of the weak interaction matrix element has not yet been experimentally tested. To our knowledge, only Ref. [15] addressed this subject when analyzing the early class of experiments, which had statistically inadequate data. A number of experimental parity violations are essential for the statistical analysis to extract the root mean square value M_J of the weak mixing matrix element. In practice the parity violation measurements are feasible only near a maximum of the p -wave neutron strength function. Initially, the TRIPLE Collaboration measured PNC effects for nuclei ^{238}U [17] and ^{232}Th [18] near the maximum of the $4p$ neutron strength function. Here we report on the PNC measurement for cadmium—our first target from the mass region near the $3p$ maximum of the neutron strength function.

The common method of PV study is measuring the target transmission in a longitudinally polarized beam [5]. Not all nuclei can be studied by this method, due to lack of the required quantity of target material (several kilograms). There is another method—neutron capture [19,20]—that is suitable for the study of parity violation with small targets of enriched isotopes. For any nonfissionable heavy nucleus, the total width of low-energy p -wave resonances is $\Gamma = \Gamma_n + \Gamma_\gamma \approx \Gamma_\gamma$ because the neutron width is extremely weak.

Consequently $\sigma_p \approx \sigma_\gamma$ and measuring PNC asymmetries in the total capture cross section and by the transmission method are equivalent ways to study parity nonconservation in the neutron p -wave resonances. We applied the capture method to the target cadmium, which was of particular interest because the first enhancement of parity violation in the compound nucleus [21] was observed in the asymmetry of the γ -ray yield following capture of polarized thermal neutrons by cadmium. For single resonances, the PNC asymmetry was already measured in ^{113}Cd [22] at $E_p = 7.0$ eV and in ^{111}Cd [5] at $E_p = 4.53$ eV. Detailed neutron spectroscopic measurements on many p -wave and s -wave resonances in ^{113}Cd were performed at the ORELA pulsed neutron source [23]. Spins of neutron p -wave and s -wave resonances of ^{113}Cd were determined recently at the GELINA pulsed neutron source [24]. Less detailed spectroscopic data are compiled by Divadeenam, Mughabghab, and Holden [25].

In Sec. II the experimental methods are described for measurements of parity violation via longitudinally polarized neutron capture. Data analysis and results for parity violating asymmetries for studied p -wave resonances are presented in Sec. III. In Sec. IV the value of the root-mean-squared matrix element $M_{J=1}$ is obtained from the measured longitudinal asymmetries for $J=1$ levels in ^{113}Cd using the likelihood analysis with probability density functions developed recently in Ref. [26] for the target spin $I \neq 0$ nuclei. Section V provides a brief summary.

II. EXPERIMENT

The PNC experiment was performed with the longitudinally polarized pulsed neutron beam available at the Los Alamos Neutron Scattering Center (LANSCE). LANSCE uses the 800-MeV proton beam from the former Los Alamos Meson Physics Facility linac. The proton beam consists of 650 μs long pulses separated by 50 ms. Each pulse is injected into and accumulated by a storage ring that compresses the pulse width from 650 μs to 125 ns [full width at half maximum (FWHM)]. After compression, the pulses are extracted from the ring and transported to a tungsten target where they produce spallation neutrons. The neutrons are moderated by slabs of water (or liquid hydrogen) and collimated into several beams with different flight paths. A more detailed description of the target-moderator geometry and performance can be found in Ref. [27], and references therein. The unpolarized neutron intensity at flight path 2, used by the TRIPLE Collaboration, is approximately given (at 70 μA average proton beam current) by $dN/dE = 2 \times 10^{12} E^{-0.96} f \Omega$ (eV s^{-1}), where Ω is the detector solid angle in steradians and f is the fraction of the $13 \times 13 \text{ cm}^2$ moderator viewed by the collimator system. This is the initial intensity without any material in the beam. The neutron beam flux was monitored by a ^3He -ionization chamber located at the exit of the bulk shield surrounding the neutron production target.

The neutron beam is polarized by spin-dependent transmission through a polarized proton target. The polarization apparatus has been described in Ref. [28] and in earlier publications of the TRIPLE Collaboration. Since then several major improvements have been made including installation of a new polarizer and extension of the spin transport system

along the flight path to 60 m where the capture detector is located. As described by Penttilä *et al.* in Ref. [29], the protons in the NH_3 target, maintained at a temperature of 1 K in a 5 T magnetic field, are polarized using the dynamic nuclear polarization technique by microwave pumping at frequency 140 GHz. The neutron beam polarization f_n is related to the polarization of the proton spin filter f_p :

$$f_n = \tanh(f_p n \sigma_{\text{pol}} t), \quad (2.1)$$

where n is the number density of protons in the target, σ_{pol} is the polarization cross section, and t is the thickness of the filtering material. The polarized beam has a diameter of 80 mm after leaving the proton cryostat. A neutron beam polarization up to 70% was achieved with a factor of 7 reduction in intensity.

The neutron spin can be reversed either by reversing the spin of the proton polarizer or by adiabatic passage through a region of spatially changing magnetic field in a spin flipper described by Bowman *et al.* [30]. The former process is rather slow, taking about an hour, and therefore the proton polarization is only reversed every one to two days. The spin flipper is used for more rapid reversals by changing the direction of the current in a transverse coil every 10 s, in a sequence chosen to minimize false asymmetries (to first order in the effects of stray fields from the transverse coil and to first and second order in effects due to time drifts in the detector). The data are sorted into good and bad data areas based on the stability of the beam during each eight-step sequence. If the total number of counts in any storage ring pulse out of 1600 in a sequence differs more than 8% from the mean, then the sequence is routed to the bad area. A run consisted of 20 sequences, taking about 30 min. Altogether 271 runs were taken on the ^{113}Cd sample.

The TRIPLE design for a multisegmented capture detector made of CsI(pure) material is described in Ref. [31]. In the present ^{113}Cd experiment, a temporary detector system was used. The detector consisted of eight $15 \times 15 \text{ cm}^2$, 15 cm thick cubic BaF_2 crystals each located ≈ 12 cm from the sample. The detector was shielded from the scattered neutrons by a hollow cylinder 5 cm thick made of 10% ^6Li -loaded polyethylene. The outside shield consisted of 10 cm lead and a 15 cm thick outer layer of 5% B-loaded polyethylene. The anode signals from the photomultiplier tubes were clipped at 25 ns, discriminated at the level of 0.5 MeV, and introduced into a coincidence logic unit. The data acquisition system, which utilized a Canberra multiscaler and 8192 channel memory, was set up with a 200 ns channel width and the information was recorded on a VAXstation II/GPX computer. A typical time-of-flight spectrum with the ^{113}Cd sample is shown in Fig. 1. The strongest s -wave resonances saturated the measuring system due to the high instantaneous count rate. However, for the p -wave resonances the detector was in the linear regime.

The isotopic sample was a highly enriched (93.35%) ^{113}Cd disc with a 90 mm diameter and total weight of 91.2 g. The sample was obtained from the Russian State Pool of Isotopes via the JINR in Dubna. Other isotopes present in the sample are ^{110}Cd (0.138%), ^{111}Cd (0.264%), ^{112}Cd (2.64%), ^{114}Cd (3.11%), and ^{116}Cd (0.208%). The abundances of the isotopes ^{106}Cd and ^{108}Cd are less than 0.01%. The areal den-

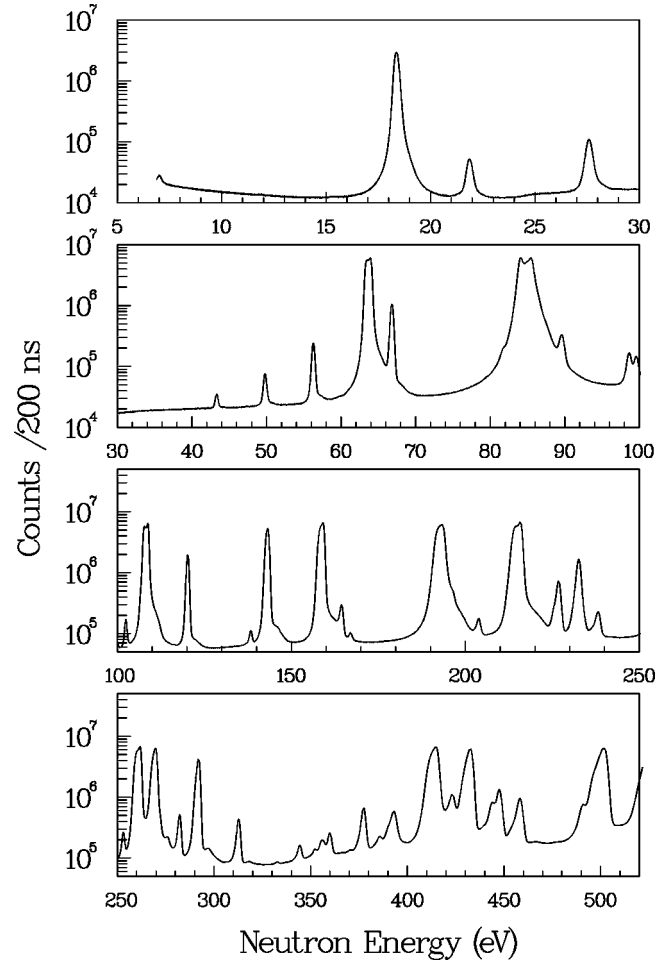


FIG. 1. ^{113}Cd neutron capture data obtained at LANSCE (logarithmic scale).

sity of the sample was 0.00764 atoms/b. The areal density of the transmission sample of natural cadmium was $n = 3.93 \times 10^{23}$.

III. DATA ANALYSIS AND RESULTS

A. Parity-violating capture asymmetries

Only the good data (as described in Sec. II A) were used in the analysis for PNC asymmetries. The data runs were further sorted off-line based on the flip to no-flip ratio R (defined as the ratio of the yield with spin reversed to the yield with spin unchanged) of total counts in the unsaturated portion of the spectrum. The beam monitor ratio was very close to one over the entire data set ($\langle R_{\text{mon}} \rangle = 0.99998 \pm 0.00005$), including rejected runs for which the TOF spectra displayed an anomalous ratio. The resulting filtered data set consisted of 216 runs. The no-flip histogram of this summed data set was normalized to the flip histogram by the mean value of the ratio $R = 1.000589$. The validity of this normalization procedure was checked by calculating the asymmetry for 12 different regions of the spectrum away from resonances. These asymmetries are consistent with zero, with the mean asymmetry of the 12 regions being $(-0.26 \pm 1.84) \times 10^{-4}$.

The spectra were fit with a modified version of the peak fitting code NEWFIT [32]. All of the data regions were fit with

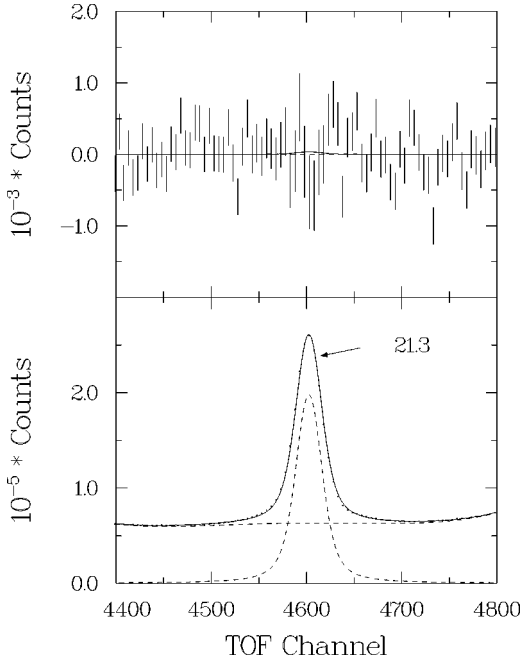


FIG. 2. Fits to the difference spectrum (top) and to the sum spectrum (bottom) near the 21.8-eV p -wave resonance. A PNC effect is not expected in this case since $J=2$; the dashed peak represents the resonance contribution after subtracting the background.

a Lorentzian convoluted with a Gaussian. Some regions also were fit with a skewed Gaussian convoluted with a Lorentzian; the skewed Gaussian more correctly reproduces the resolution function of the LANSCE moderator. Our procedure was first to obtain the line shape parameters by fitting the sum of the spectra for the \pm spin directions. These parameters were then fixed, and the difference spectrum $N^+ - N^-$ was fit varying only the peak area. The yield asymmetry $\epsilon = (N^+ - N^-)/(N^+ + N^-)$ was then calculated. Examples of fits to the sum and difference spectra are shown in Figs. 2 and 3: the resonances at 21.8 eV and 98.6 eV have spin $J=2$ and PNC effects are not expected in such a case, while the 102.3-eV p -wave resonance has spin $J=1$ and does exhibit a PNC effect. The level at 99.5 eV is an s -wave resonance of the ^{111}Cd isotope.

In another analysis, the uncertainties in the PNC asymmetries were determined by the method of replicate trials. All 216 individual runs were fit using the parameters determined in the analysis described above. The asymmetry was determined from the mean of this distribution and the uncertainty was the width of this distribution divided by \sqrt{N} , where N is the number of trials. The uncertainties determined in this way were slightly larger than those obtained in the previous analysis, while the nonzero asymmetries agree.

The final step in data analysis was the transformation of the capture yield asymmetry ϵ_γ , to the PNC asymmetry \mathcal{P} in the p -wave cross section according to the relation

$$\epsilon_\gamma = \alpha f_n \mathcal{P}, \quad (3.1)$$

where α is the correction factor accounting for neutron capture in the target after multiple scattering. For the thin ^{113}Cd sample multiple scattering effects were negligible for all p -wave resonances: $\alpha(\text{Cd}) \approx 1$. The relative neutron polar-

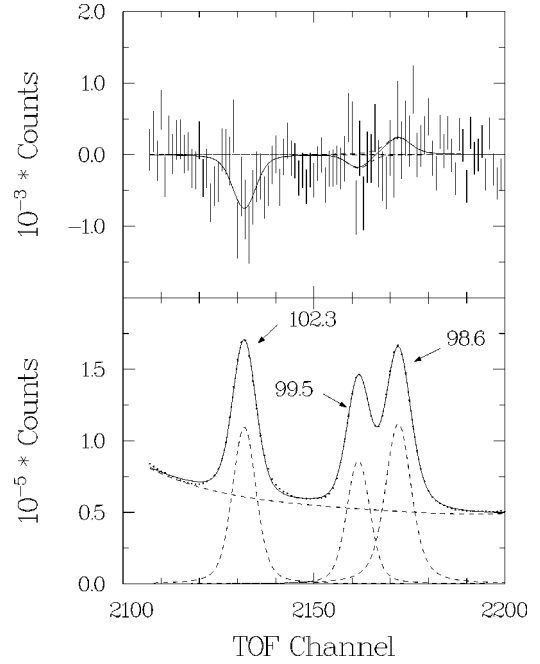


FIG. 3. Fits to the difference spectrum (top) and to the sum spectrum (bottom) near the 102.3-eV p -wave resonance which exhibits a PNC effect; the dashed resonance shapes obtained after the background subtraction are the 102.3-eV level in ^{113}Cd , the 99.5-eV s -wave level in ^{111}Cd , and the 98.6-eV level with $J=2$ in ^{113}Cd .

ization was monitored continuously by NMR measurement of the proton polarization f_p with the use of Eq. (2.1). The value of the proton NMR polarization was stored for each neutron spin sequence and averaged to produce the relative neutron polarization for each run. The absolute calibration of the neutron polarization was performed by transmission measurement of the known PNC asymmetry in the 0.74-eV resonance of ^{139}La target placed in the downstream end of the spin flipper. The average beam polarization (for the summed data set) at this 10-m position was $f_n(E_p=0.74 \text{ eV}) = 0.66 \pm 0.04$. \mathcal{P} asymmetries were extracted for 23 p -wave resonances in ^{113}Cd listed in Table I. The uncertainties quoted are the statistical, peak fitting, and the beam polarization errors combined. The energies were calibrated to the resonance energies determined in Ref. [23]. The parity assignments for the majority of cases are taken from Ref. [23]. Resonances at energies 281.8 and 457.8 eV, quoted in Ref. [23] as s waves on the basis of probabilistic arguments, are assigned here as p -wave resonances on the basis of the γ -ray spectra [24]. The shape analysis of the present sum data near 290 eV gave no direct indication of the presence of the weak 289.64-eV level as found in ORELA measurement [23] on the tail of the s -wave resonance 291.61 eV. The poorer TOF resolution of our experiment (2 eV for one channel at $E=290$ eV) did not allow these peaks to be resolved. However, we did see a statistically significant PV effect over the peak observed near 291 eV. We renormalized the observed parity violating effect to the \mathcal{P} value for 289.64-eV resonance presented in Table I using the $g\Gamma_n$ data from Ref. [23].

It is possible that the cumulative effect of multiple gaps in the spin transport system coupled with the Earth's magnetic

TABLE I. Capture PNC asymmetries and parameters of the p -wave resonances in ^{113}Cd

E_n (eV)	J^a	$g\Gamma_n$ (meV) ^b	\mathcal{P} (%)
7.00±0.01	1	0.00031±0.00003	-0.80±0.36
21.83±0.01	2	0.0071±0.0002	-0.04±0.22
43.38±0.03	0	0.0047±0.0004	-0.32±0.55
49.77±0.01	1	0.0150±0.0005	-0.05±0.22
56.23±0.01	2	0.0403±0.0006	+0.23±0.10
81.52±0.01		0.0052±0.0006	+0.56±1.15
98.52±0.02	2	0.042±0.001	-0.33±0.21
102.30±0.02	1	0.037±0.001	+1.04±0.22
106.56±0.02		0.030±0.002	
166.60±0.13		0.020±0.002	+2.00±1.10
196.15±0.04		0.100±0.005	-1.65±0.76
203.51±0.04	1	0.067±0.003	-0.50±0.40
211.88±0.05		0.078±0.003	
237.87±0.05	2	0.125±0.004	+0.24±0.21
252.68±0.05	2	0.140±0.004	+0.25±0.25
271.50±0.06		0.26±0.01	
281.83±0.06	1	0.48±0.01	-0.20±0.14
289.64±0.09	(1) ^c	0.06±0.006	+5.1±1.1
312.30±0.07	2	0.491±0.007	+0.16±0.15
343.79±0.07	0	0.17±0.01	-0.41±0.51
351.6±0.2	2	0.036±0.003	-0.46±1.24
359.3±0.1	1	0.28±0.01	-0.22±0.34
376.8±0.1	1	0.83±0.01	-0.33±0.13
385.0±0.1		0.089±0.006	-0.18±0.61
422.7±0.1	2	1.00±0.02	
457.8±0.1	1	1.62±0.02	-0.05±0.10
489.9±0.1	1	0.72±0.02	+0.04±0.23

^aSpins taken from Ref. [24].

^bValues taken from Ref. [23].

^cSpin deduced from the presence of PV.

field could reduce the polarization of the beam at the 60-m sample position. According to calculations in Ref. [33], the depolarization (defined as the relative difference of beam polarizations at 60 and 10 m) shows fluctuating energy behavior that decreases with neutron energy. For normal conditions and for energies from about 5 to 500 eV, these fluctuations are less than 3% with an average depolarization value of about 2%. For the case of no B field in the detector section of the solenoid, as an example of abnormal conditions, a depolarization of 12% near 0.7 eV and of 2% around 100 eV was calculated. We believe that, on average, depolarization was less than 5% for energies above 7 eV. This is confirmed by our \mathcal{P} value for the 7-eV resonance, which agrees with the value 0.98 ± 0.30 in Ref. [22], and by the depolarization free transmission measurement described below.

B. Parity-violating transmission asymmetries

A transmission measurement was performed with a 8.46-cm thick natural Cd target placed in the polarized beam after the spin-flipper at 6-m position. A ^{10}B liquid scintillator detector [34] was used at 56 m. This transmission measurement, initially intended to verify the capture value of \mathcal{P} at the

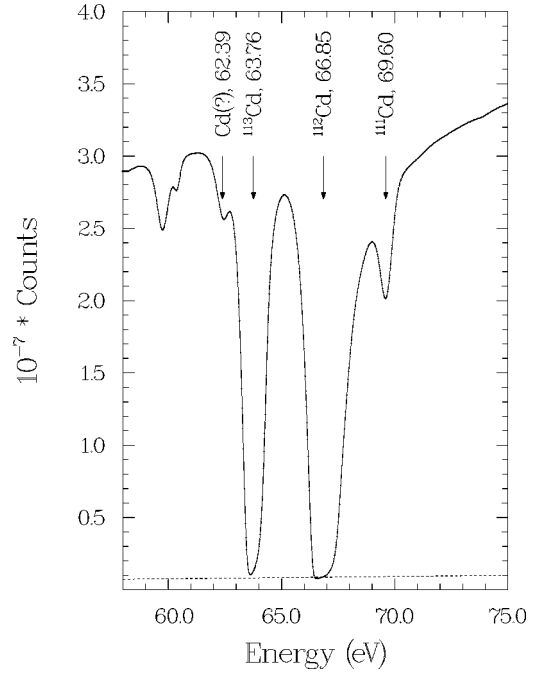


FIG. 4. The experimental (points) and fitted (full line) Cd sample-in transmission spectra in the 60–73 eV energy range. The dashed line is the background.

102.3-eV resonance, revealed two more cases of parity violation in cadmium. A count rate asymmetry ϵ in a transmission experiment bears a different relationship to the cross section asymmetry \mathcal{P} than in the capture case [Eq. (3.1)]. Here [5,8]

$$\epsilon(E) = -\tanh[n\sigma(E)f_n\mathcal{P}], \tag{3.2}$$

which involves the resonance parameters describing the cross section $\sigma(E)$ defined by Eq. (1.2). For p -wave resonances, the $n\sigma(E)$ value is small even for thick samples [$n\sigma(E) < 1$], and the Doppler broadening and the instrumental resolution function additionally reduce the value of $\sigma(E)$ and, therefore, the experimental value of ϵ . As opposed to the capture case, it is not straightforward to deduce the asymmetry \mathcal{P} from the “observed” value $\langle\epsilon\rangle$ calculated as the relative difference of the corresponding count rate sums over the resonance. In particular, there are difficulties in the case of weak levels in the vicinity of strong ones. Consequently, it is best to fit the summed (+ and - helicities) spectra first to obtain the resonance and resolution function parameters and then fit the + and - spectra separately to obtain \mathcal{P} . This procedure was performed on the natural cadmium data with the fitting code FITXS developed in Ref. [35]. The code implements the Reich-Moore multilevel cross section formalism and takes full account of the LANSCE time-of-flight spectrometer resolution function. As an example, the sample-in data fit (80 runs) in the 60–73 eV range is shown in Fig. 4. Fits for the energy range around 102 eV are shown in Figs. 5 and 6. The p -wave 102.30-eV resonance of ^{111}Cd is between 99.50-eV and 103.05-eV s -wave resonances of ^{111}Cd . To show its presence and size, the contribution of the 102.30-eV level to the fit shown in Fig. 5 is omitted and the result is shown in Fig. 6. Some transmission results are presented in Table II. The values of $\langle\epsilon\rangle$ are

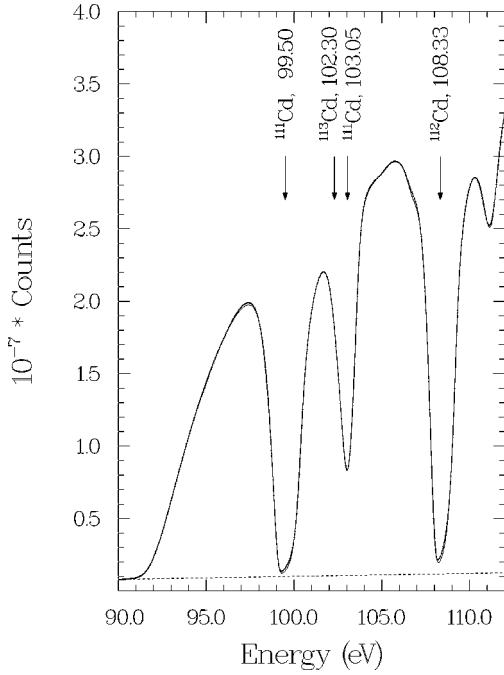


FIG. 5. The experimental and fitted Cd sample-in transmission spectra around 102 eV: all levels are taken into account. The dashed line is the background.

listed to demonstrate the small size of observables in this transmission experiment as compared with \mathcal{P} . The neutron widths were in agreement with Refs. [25,23] except for the 102.30-eV resonance for which the initial fit gave a value of 0.090 meV instead of the known value 0.037 meV. However, it was found that addition of the p -wave resonance (supposedly of ^{111}Cd) at the energy 102.54 eV led to agreement. The values $E_n = 102.54$ eV and $g\Gamma_n = 0.054$ meV of this new resonance were determined from fits keeping the values of

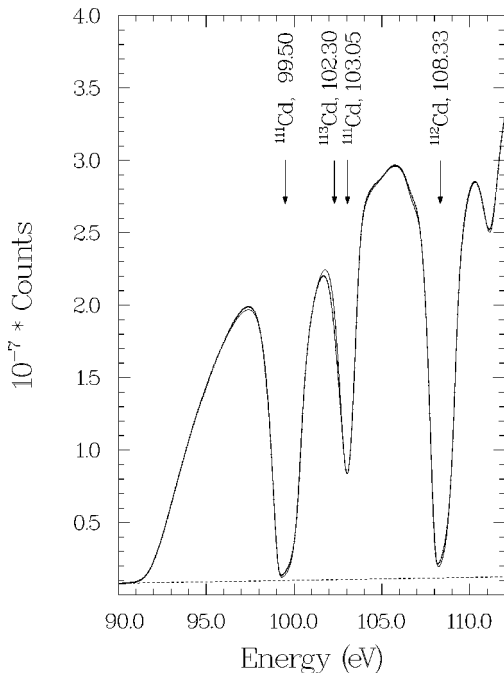


FIG. 6. Same as Fig. 4 but the 102.30-eV resonance is omitted in the plot.

the $E = 102.30$ eV resonance parameters fixed as given in Ref. [23]. With these parameters, the transmission value of \mathcal{P} for the 102.30-eV resonance agrees with the capture value of \mathcal{P} within statistical uncertainty. A tentative ^{111}Cd isotopic assignment for the parity violating 62.39-eV resonance needs experimental confirmation. Nevertheless, we believe that we discovered two more cases of parity violation in ^{111}Cd : 62.39-eV and 69.60-eV resonances—in addition to the previously known case of the 4.53-eV resonance [5].

IV. WEAK MATRIX ELEMENT

All previous experimental work on the rms matrix element M_J involved target nuclei with $I=0$. There parity violation occurs for the spin $J=1/2$ resonances, and since for such a case $g_{p(3/2)}=0$, the parameter R in Eq. (1.3) has the value $R=1$ and the asymmetry \mathcal{P} is in fact a sum of Gaussian variables V_{sp} with constant coefficients

$$A_{sp} = \frac{2g_s(E_p)/g_p(E_p)}{E_s - E_p}. \quad (4.1)$$

Such quantity is Gaussian with variance $A_p^2 M_J^2$, where

$$A_p = \sqrt{\sum_s A_{sp}^2}. \quad (4.2)$$

As emphasized in the Introduction, it is possible then to obtain M_J by the likelihood analysis of measured asymmetries $\mathcal{P}(E_p)$, which was performed for the first time in Ref. [8]. The quantity A_p^2 involves only experimentally known neutron resonance parameters; the signs of the neutron width amplitudes do not enter. To include experimental errors σ in \mathcal{P} , the convolution theorem is used with the result that the probability density function for \mathcal{P} is Gaussian with variance $(A_p^2 M_J^2 + \sigma^2)$ [8].

The extension of the method to targets with spin $I \neq 0$ is discussed in Ref. [26]. The method can be identified as a Bayesian method with uniform prior probability. We perform the data analysis in terms of the likelihood function $L(M_J)$ originated as the post probability function $P(M|\mathcal{P})$ in the frame of Bayes theorem

$$L(M_J) \equiv P(M_J|\mathcal{P}) = \frac{P(\mathcal{P}|M_J)P(M_J)}{P(\mathcal{P})}, \quad (4.3)$$

with $P(\mathcal{P}) = \int P(\mathcal{P}|M_J)P(M_J)dM_J$. As usual, a constant-valued *a priori* function $P(M_J)$ for a parameter M_J is in use for situations where nothing is known *a priori* about the parameter M_J . The overall normalization constant $P(M_J)/P(\mathcal{P})$ in Eq. (4.3) is calculated by integrating $P(M_J|\mathcal{P})$ over M_J . The explicit forms of the likelihood functions used by different authors in analysis of PV data are discussed elsewhere [36]. For $I \neq 0$ targets and the case of complete knowledge of spins and other parameters including the amplitudes $g_{1/2}$ and $g_{3/2}$, the extension is trivial: one introduces the reduced observable $\mathcal{P}/A_p R$, for which the probability function is Gaussian with variance M_J^2 . In other words, the experimental asymmetry \mathcal{P} follows a Gaussian distribution with variance $(M_J^2 A_p^2 R^2 + \sigma^2)$. In our case of ^{113}Cd , neutron widths and spin are known. However, the

TABLE II. PNC transmission asymmetries and parameters of some resonances in Cd.

E_n (eV)	A	$g\Gamma_n$ (meV)	$g\Gamma_n$ (meV) ^a	$10^4\langle\epsilon\rangle$	$\mathcal{P}(\%)$
62.39	(111)	0.026±0.002	0.042±0.019	7.9±0.4	1.12±0.07
63.76	113	2.10±0.17	2.6±0.1		
66.85	112	7.0±0.4	7.5±1.0		
69.60	111	0.070±0.005	0.10±0.02	1.6±0.4	0.13±0.03
89.50	110	132±6	130±10		
99.50	111	9.0±0.6	10±1		
102.30	113	0.037±0.001	0.037±0.001	2.4±0.7	0.83±0.20
102.54	(111)	0.054±0.003			
103.05	111	0.65±0.05	0.75±0.10		
291.61	113	4.40±0.07	4.40±0.07		

^aValues taken from Refs. [23,25].

p -wave amplitudes $g_{p(1/2)}$ and $g_{p(3/2)}$ are unknown. In this case the quantity R in Eq. (1.3) must be treated as a random variable, so that the asymmetry \mathcal{P} is the product $\mathcal{P}=GR$ of the Gaussian variable $G=\sum_s 2V_{sp}g_s/[E_s-E_p]g_p$ and a random variable R . The latter is a known function of the two Gaussian variables $g_{p(1/2)}$ and $g_{p(3/2)}$ with the variances $\langle g_{p(1/2)}^2 \rangle$ and $\langle g_{p(3/2)}^2 \rangle$ correspondingly. The resulting probability density function of \mathcal{P} is no longer Gaussian. As shown in Ref. [26], it is

$$P(\mathcal{P}|M_J A_p, a, \sigma) = \frac{2}{\pi} \int_0^{\pi/2} \frac{a}{a^2 \sin^2 \theta + \cos^2 \theta} \frac{d\theta}{\sqrt{2\pi(M_J^2 A_p^2 \sin^2 \theta + \sigma^2)}} \times \exp\left(-\frac{\mathcal{P}^2}{2(M_J^2 A_p^2 \sin^2 \theta + \sigma^2)}\right), \quad (4.4)$$

where θ is defined through $\tan \theta = g_{p(1/2)}/g_{p(3/2)}$. The parameter a^2 is $a^2 \equiv \langle g_{p(3/2)}^2 \rangle / \langle g_{p(1/2)}^2 \rangle$, its value can be obtained from data on the $p_{3/2}$ and $p_{1/2}$ neutron strength functions. For small a this function is Gaussian and is identical to the target spin $I=0$ function, since then $R=1$. The shape of $P(\mathcal{P}|M_J A_p, a, \sigma)$ for large values of \mathcal{P} remains approximately Gaussian. The effect of the appearance of a $p_{3/2}$ amplitude in the neutron width is to produce a spike near $\mathcal{P}=0$ at the expense of large values of \mathcal{P} .

This probability density function was used to construct the Bayesian likelihood function $L(M_J)$ with uniform prior probability

$$L(M_J) = N_0 \prod_{i=1}^{10} P(M_J | \mathcal{P}_i, A_p, a, \sigma_i), \quad (4.5)$$

where N_0 is a normalization constant and the product is over the data for the ten spin $J=1$ p -wave resonances in ¹¹³Cd with measured \mathcal{P} . This likelihood function has an asymmetric shape that leads to asymmetric error bars for M_J . The M_J values are obtained by finding the value of M_J^* that maximizes $L(M_J)$. A confidence interval for M_J is obtained by solving the equation

$$\ln \left[\frac{L(M_J^\pm)}{L(M_J^*)} \right] = \frac{1}{2}. \quad (4.6)$$

The obtained result for the weak matrix element in ¹¹³Cd is

$$M_{J=1} = 2.9_{-0.9}^{+1.3} \text{ MeV}. \quad (4.7)$$

The given value of the matrix element is influenced considerably by the PV value for the 289.64-eV resonance, which alone contributes 1.6 meV. The small width of this resonance is exactly the source of the large contribution to the matrix element: \mathcal{P} is large because the denominator in Eq. (1.1) is small. The inclusion of the 289.64-eV result in the analysis to extract $M_{J=1}$ is justified since the experimental asymmetry at an energy about 291 eV is unambiguous. The data of Ref. [23] are clear in the existence of two resonances at this energy, one of which is a p wave. Since PV effects are measurable only in p -wave resonances, our decision to normalize the asymmetry to the p -wave cross section, which results in the large asymmetry \mathcal{P} , is the only logical course if our data and the data of Ref. [23] are taken at face value. We are aware of possible doubts in the merit of the given uncertainty in $M_{J=1}$. In this connection we would like to draw the attention of readers to the Flambaum and Gribovskii [38] conjecture that PV effects do not obey the central limit theorem of probability theory, therefore, large fluctuations are expected and the effects in few resonances might dominate the mean value.

The likelihood function can be expressed as a function of the weak spreading width through Eq. (1.4). A plot of the ¹¹³Cd likelihood function calculated with the p -wave data from Table I, the s -wave data from Ref. [23], spins from Ref. [24], and the value $a=0.7$ from Ref. [37] is given in Fig. 7. The most likely value of the spreading width is

$$\Gamma_w = (16.2_{-8.3}^{+17.7}) \times 10^{-7} \text{ eV}. \quad (4.8)$$

It was calculated with the value $D_{J=1} = 33 \pm 4$ eV which follows from the ‘‘observed’’ value $D_{\text{obs}} = 24.8 \pm 2.6$ eV [23] after applying the $(2J+1)$ -law of spin dependence of level densities. The ¹¹³Cd weak spreading width can be compared with the value $\Gamma_w = 5.5_{-3.0}^{+5.6}$ in Ref. [18] for ²³²Th and with the value $\Gamma_w = 0.9_{-0.5}^{+1.9}$ in Ref. [17] for ²³⁸U (in the same units of 10^{-7} eV). There is little evidence for a mass dependence of the weak spreading width. The experimental value of the weak matrix element given by Eq. (4.7) agrees well with an estimate $M_J = 2.0$ meV from Eq. (1.5). However, the results are not precise enough to distinguish between the

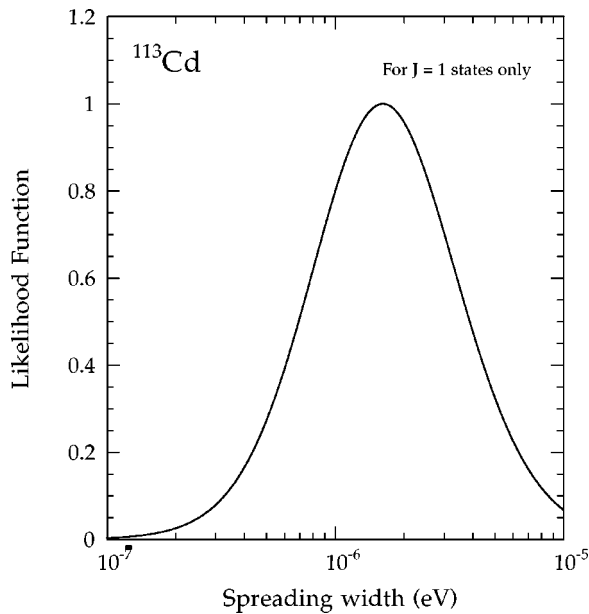


FIG. 7. The likelihood function for the weak matrix element M in ^{113}Cd calculated from longitudinal asymmetries of the 10 p -wave resonances with $J=1$.

different approaches to the mass dependence of M_J discussed in Sec. I. PNC asymmetry measurements for additional nuclei in the mass region $A \approx 100$, as well as from other regions, are necessary to determine the mass dependence of the weak spreading width.

V. SUMMARY

We performed capture measurements of PNC longitudinal asymmetries in ^{113}Cd in the neutron energy region 7–500 eV. These measurements are equivalent to transmission experiments, in the sense that both measure the parity violating part of the total resonance cross section. The capture technique using a nearly 4π detector has a sensitivity advantage, which makes possible PNC measurements with small samples of enriched isotopes. Of the 23 p -wave resonances

studied in ^{113}Cd , four resonances showed parity violation with greater than 2.2σ statistical significance. Only about one half of the cadmium resonances can exhibit parity violation, namely those with spins $J=0$ or 1 but not those with $J=2$. We used the J values determined in Ref. [24]. The two $J=0$ resonances showed no parity violation at the accuracy level 5×10^{-3} . The sample of ten resonances with $J=1$ was analyzed to determine $M_{J=1}$. The value obtained, $M_{J=1}(^{113}\text{Cd}) = 2.9^{+1.30}_{-0.9}$ meV, is the first experimental value of M_J for nuclei in the region of the $3p$ maximum of the neutron p -wave strength function $A \approx 100$. The value of the weak spreading width is not very different from the values for uranium and thorium nuclei from the $4p$ -maximum region, implying that the spreading width of the weak interaction in nuclei has the same order of magnitude.

There remain unresolved issues. The uncertainty in the M_J values is not small enough to distinguish between different theoretical predictions for the mass dependence of M_J . We plan to measure PNC asymmetries for other nuclei in the $A \approx 100$ mass region in order to improve the precision of M_J . These measurements will be performed with both transmission and capture techniques, and with the new polarization setup which was used in this experiment. For capture measurements a new 4π detector with 24 CsI(pure) crystals is assembled and tested. Resonance spin determination on other target candidates for PNC study would be of great value.

ACKNOWLEDGMENTS

The authors would like to thank C. D. Bowman, G. T. Garvey, and V. I. Furman for valuable discussions. The authors thank C. L. Morris for making available and helping to modify the code NEWFIT for this application. The work of the Geel group on the spins of ^{113}Cd resonances is greatly acknowledged. This work was supported in part by the U.S. Department of Energy, Office of High Energy and Nuclear Physics, under Grant Nos. DE-FG02-97ER41042 and DE-FG02-97ER41033 and by the U.S. Department of Energy, Office of Energy Research, under Contract No. W-7405-ENG-36.

-
- [1] V. P. Alfimenkov, Usp. Fiz. Nauk **144**, 361 (1984) [Sov. Phys. Usp. **27**, 797 (1984)].
- [2] J. D. Bowman, *Parity and Time Reversal Violation in Compound Nuclear States and Related Topics*, edited by N. Auerbach and J. D. Bowman (World Scientific, Singapore, 1996), p. 65.
- [3] J. D. Bowman, G. T. Garvey, Mikkel B. Johnson, and G. E. Mitchell, Annu. Rev. Nucl. Part. Sci. **43**, 829 (1993).
- [4] C. M. Frankle, S. J. Seestrom, Yu. P. Popov, E. I. Sharapov, and N. R. Roberson, Fiz. Elem. Chastits At. Yadra **24**, 939 (1993) [Sov. J. Part. Nucl. **24**, 401 (1993)].
- [5] V. P. Alfimenkov, S. B. Borzakov, Vo Van Thuan, Yu. D. Mareev, L. B. Pikelner, A. S. Khrykin, and E. I. Sharapov, Nucl. Phys. **A398**, 93 (1983).
- [6] V. V. Flambaum and O. P. Sushkov, Nucl. Phys. **A412**, 13 (1984).
- [7] V. E. Bunakov and V. P. Gudkov, Nucl. Phys. **A401**, 93 (1983).
- [8] J. D. Bowman *et al.*, Phys. Rev. Lett. **65**, 1192 (1990).
- [9] V. E. Bunakov, E. D. Davis, and H. A. Weidenmüller, Phys. Rev. C **42**, 1718 (1990).
- [10] E. D. Davis, Z. Phys. A **340**, 159 (1991); **340**, 310 (1991).
- [11] J. B. French, V. K. B. Kota, A. Pandey, and S. Tomsovic, Ann. Phys. (N.Y.) **181**, 235 (1988).
- [12] H. L. Harney, A. Richter, and H. A. Weidenmüller, Rev. Mod. Phys. **58**, 607 (1986).
- [13] N. Auerbach, Phys. Rev. C **45**, R514 (1992).
- [14] S. G. Kadenskii, V. P. Markushev, and V. I. Furman, Yad. Fiz. **37**, 277 (1983) [Sov. J. Nucl. Phys. **37**, 345 (1983)].
- [15] V. E. Bunakov, V. P. Gudkov, S. G. Kadenskii, I. A. Lomachenkov, and V. I. Furman, Yad. Fiz. **49**, 988 (1989) [Sov. J. Nucl. Phys. **49**, 613 (1989)].

- [16] A. Gilbert and A. G. W. Cameron, *Can. J. Phys.* **43**, 1146 (1965).
- [17] X. Zhu *et al.*, *Phys. Rev. C* **46**, 768 (1992).
- [18] C. M. Frankle *et al.*, *Phys. Rev. C* **46**, 778 (1992).
- [19] Y. Masuda, T. Adachi, A. Masaike, and K. Morimoto, *Nucl. Phys.* **A478**, 737c (1988).
- [20] E. I. Sharapov, S. A. Wender, H. Postma, S. J. Seestrom, C. R. Gould, O. A. Wasson, Yu. P. Popov, and C. D. Bowman, *Capture Gamma-Ray Spectroscopy*, edited by R. W. Hoff (AIP, New York, 1991), p. 756.
- [21] Yu. G. Abov, P. A. Krupchitsky, and Yu. A. Oratovsky, *Phys. Rev. Lett.* **12**, 25 (1964).
- [22] V. P. Alfimenkov, Yu. D. Mareev, L. B. Pikelner, V. R. Skoy, and V. N. Shvetsov, *Yad. Fiz.* **54**, 1489 (1991) [*Sov. J. Nucl. Phys.* **54**, 907 (1991)].
- [23] C. M. Frankle, E. I. Sharapov, Yu. P. Popov, J. A. Harvey, N. W. Hill, and L. W. Weston, *Phys. Rev. C* **50**, 2774 (1994).
- [24] F. Gunsing, F. Corvi, K. Athanassopoulos, H. Postma, Yu. P. Popov, and E. I. Sharapov, *Phys. Rev. C* **56**, 1641 (1997).
- [25] S. F. Mughabhab, M. Divadeenam, and N. E. Holden, *Neutron Cross Sections* (Academic, New York, 1991), Vol. 1A.
- [26] J. D. Bowman, L. Y. Lowie, G. E. Mitchell, E. I. Sharapov, and Yi-Fen Yen, *Phys. Rev. C* **53**, 285 (1996).
- [27] P. W. Lisowski, C. D. Bowman, G. J. Russell, and S. A. Wender, *Nucl. Sci. Eng.* **106**, 208 (1990).
- [28] N. R. Roberson *et al.*, *Nucl. Instrum. Methods Phys. Res. A* **326**, 549 (1993).
- [29] S. I. Penttilä, J. D. Bowman, P. P. J. Delheij, C. M. Frankle, D. G. Haase, R. Mortensen, H. Postma, S. J. Seestrom, and Y.-F. Yen, *Time Reversal Invariance and Parity Violation in Neutron Reactions*, edited by C. R. Gould, J. D. Bowman, and Yu. P. Popov (World Scientific, Singapore, 1994), p. 198.
- [30] J. D. Bowman, S. I. Penttilä, and W. B. Tippens, *Nucl. Instrum. Methods Phys. Res. A* **369**, 195 (1996).
- [31] C. M. Frankle, J. D. Bowman, S. J. Seestrom, N. R. Roberson, and E. I. Sharapov, *Time Reversal Invariance and Parity Violation in Neutron Reactions* [29], p. 204.
- [32] C. L. Morris, Program NEWFIT, 1993 (unpublished).
- [33] B. E. Crawford, PhD Thesis, Duke University, 1997.
- [34] Yi-Fen Yen *et al.*, *Time Reversal Invariance and Parity Violation in Neutron Resonances* [29], p. 210.
- [35] J. D. Bowman, Y. Matsuda, and Y.-F. Yen (unpublished).
- [36] J. D. Bowman, E. I. Sharapov, and L. Y. Lowie, *Fiz. Elem. Chastits At. Yadra* **27**, 965 (1996) [*Sov. J. Part. Nucl.* **27**, 398 (1996)].
- [37] G. S. Samosvat, *Fiz. Elem. Chastits At. Yadra* **17**, 713 (1986) [*Sov. J. Part. Nucl.* **17**, 313 (1986)].
- [38] V. V. Flambaum and C. F. Gribakin, *Phys. Rev. C* **50**, 3122 (1994).